# Clay-Based Polymer Nanocomposites

Subjects: Nanoscience & Nanotechnology

Contributor: edgar Franco

Clay-based polymer nanocomposites are often referred to as polymer layered silicates, nanostructured polymers, or simply polymer nanocomposites. These polymers are reinforced with inorganic particles containing at least one dimension in the nanometric scale (<100 nm). Compared to traditional composites (macro- or microscale), polymer nanocomposites offer the opportunity to explore new behaviors and functionalities beyond conventional polymers. Nanoparticles often strongly influence the mechanical properties of polymers in very low volume fractions due to the relatively short distance between nanoparticles, molecular compatibility, and interfacial interaction between the particles and the polymer chains.

polymer-layered silicates | oMMT | clay minerals | mechanical properties

## 1. Clay-Based Polymer Nanocomposites

Clay minerals are known as phyllosilicates, or lamellar silicates, which are the inorganic particles most commonly used to prepare clay-based polymer nanocomposites [1][2][3]. It is necessary to highlight that the clay particles are not by themselves nanometric scale particles, but instead that they are formed by the stacking of several layers that leads to the development of irregular aggregates, as schematized in **Figure 1**. Each layer has a high aspect ratio between 100 and 800 nm in length and approximately 1 nm in thickness. Its uniform dispersion within the polymer matrix favors developing a very high interfacial area per unit volume, which is the primary reinforcement mechanism of clay-based polymer nanocomposites. However, the layer dispersion mechanism is complex since different aspects must be considered, and that is why the specialized literature focuses on evaluating processing conditions to achieve the maximum level of dispersion [1][4][5][6][7].

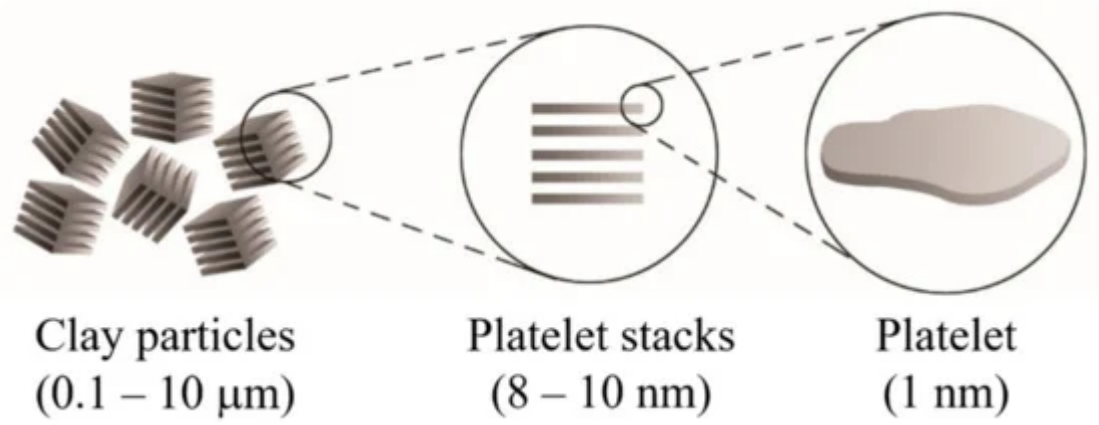


**Figure 1.** Schematic representation of the arrangement of the platelet stacks that conform to the clay particles.

Clay layers have a molecular structure based on the stacking sequence. Interesting and complete information is available on the web page of Professor Dorronsoro Fernández from the University of Granada, Spain (Department of Soil Science and Agricultural Chemistry, https://www.edafologia.net/, last visited 12 May 2021).

The basic compositional unit is the silicon–oxygen (Si-O) tetrahedron, as outlined in **Figure 2**a. It consists of one silicon cation ($Si^{-4}$) surrounded by four oxygen anions ($O^{-2}$). Chemically, the Si-O tetrahedron has a net electrical charge of −4, $(SiO_4)^{-4}$, so it is balanced by adding other cations to neutralize their charges (**Figure 3**a). For this, each vertex of the basal plane belongs to two tetrahedra, since each oxygen is in coordination with two silicones, forming tetrahedral layers distributed under the configuration of hexagons, as can be seen in detail in **Figure 4**. Sheet silicates (also called layered silicates or phyllosilicates) are obtained when three oxygens on each tetrahedron link to other tetrahedra to form tetrahedral planes.

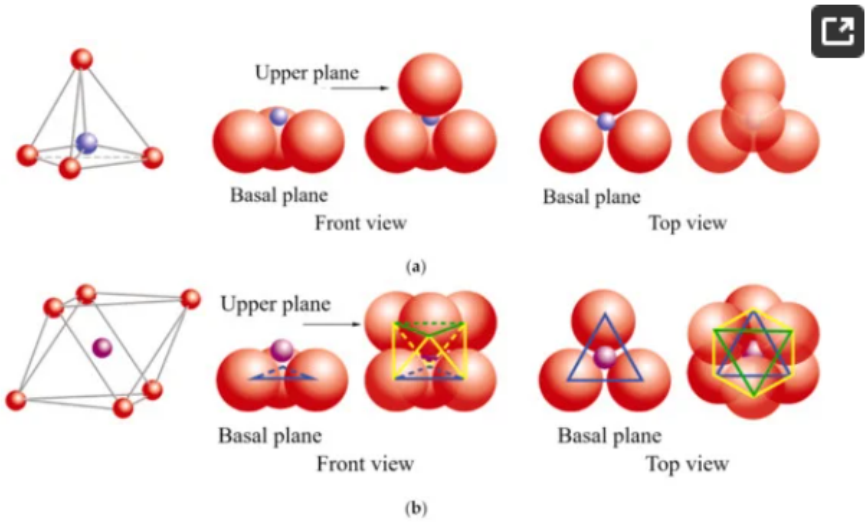


**Figure 2.** Schematic representation: (**a**) silicon tetrahedron, (**b**) magnesium and/or aluminum octahedron. In both cases, a general diagram is presented, a front view and a top view. oxygen, silicon, magnesium/aluminum. Adapted from **https://www.edafologia.net/**, last visited 12 May 2021.

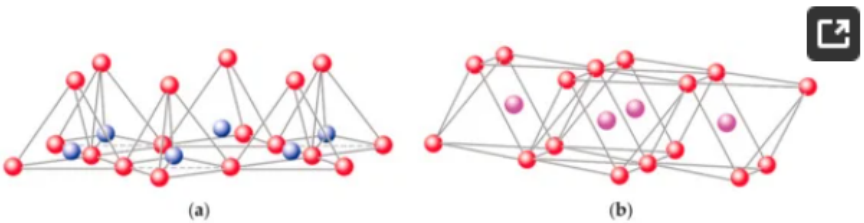


**Figure 3.** Schematic representation of the structural layers of clays: (**a**) silicon tetrahedron, (**b**) magnesium and/or aluminum octahedron. oxygen, silicon, magnesium/aluminum. Adapted from **https://www.edafologia.net/**, last visited 12 May 2021.

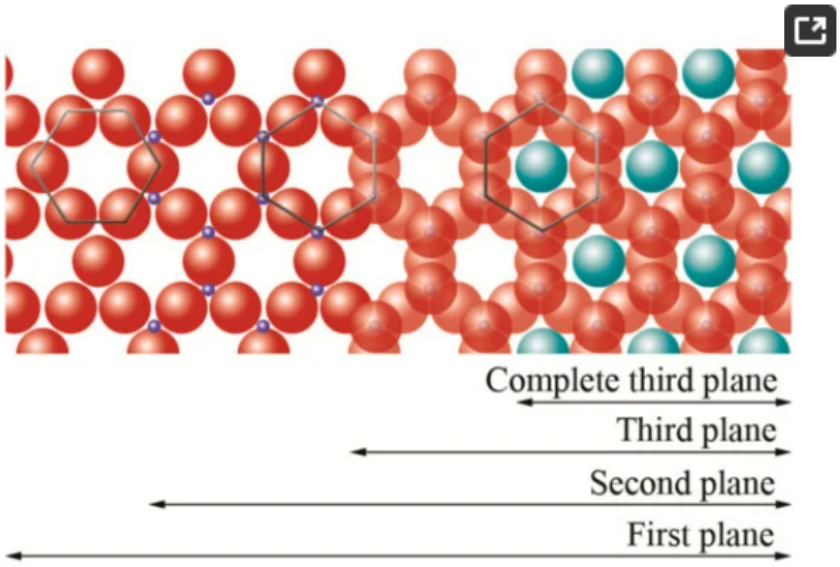


**Figure 4.** Schematic representation from the top view of the planes formed by the union of tetrahedral and octahedral layers. oxygen, silicon, hydroxyl groups. Adapted from https://www.edafologia.net/, last visited 12 May 2021.

Sheet silicates are planar structures containing different kinds of layer that can accommodate cations of all sizes. Tetrahedral layers (labeled T in this work) consist primarily of $SiO_4$ tetrahedra. Octahedral layers (labeled O in this work) contain divalent and trivalent cations ($Mg^{2+}$ or $Al^{3+}$) in 6-fold coordination, where each octahedron is supported on one of its faces, which represents the octahedral basal plane, as schematized in **Figure 2**b. Octahedral sheets are composed of individual octahedrons that share edges composed of oxygen and hydroxyl anion groups, with Mg or Al typically serving as the coordinating cation, as presented in **Figure 3**b. In two dimensions, anions can fit together in symmetrical patterns to form hexagonal patterns (**Figure 4**).

In three dimensions, tetrahedral (T) and octahedral (O) layers may stack in various ways. The arrangement of both layers can be better understood if they are represented through atomic planes, as outlined in **Figure 5**.

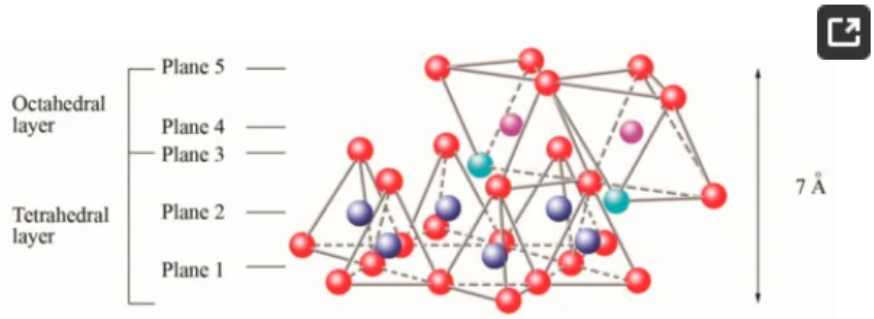


**Figure 5.** Schematic representation of the final structure corresponding to sheet 1:1. oxygen, silicon, magnesium/aluminum, hydroxyl groups. Adapted from [9].

The first plane corresponds to the basal plane of the tetrahedral layer. Silicon atoms are placed in the second plane, occupying part of the space in the basal plane of each tetrahedron (**Figure 4**). In a third plane, the unshared oxygens (also called apical oxygen) are located just above the silicon, ending up occupying the remaining space, as depicted in **Figure 4**. In this way, the arrangement of these three planes constitutes the fundamental unit of the tetrahedral layers (**Figure 5**).

The union between tetrahedral and octahedral sheets occurs with the apical oxygen, linked to $Mg^{2+}$ or octahedral $Al^{3+}$. However, not all the vertices of the octahedral basal plane, formed in part by the apical oxygen, would be shared with the silicon atoms contained in the tetrahedra, so the charge balance occurs when they bind to a hydrogen atom (H), forming hydroxyl groups (OH), as shown in **Figure 4** and **Figure 5**. Thus, the basal plane of the octahedron forms part of the superior plane of the tetrahedra and completes the third plane. It should be noted that all planes represent a hexagonal lattice, while the third plane forms a centered hexagonal lattice, as shown in **Figure 4**.

The fourth plane consists of the arrangement of octahedral $Mg^{2+}$ or $Al^{3+}$ atoms. These atoms are located in the small free spaces left by every two apical oxygens and one OH group, as shown in **Figure 6**.

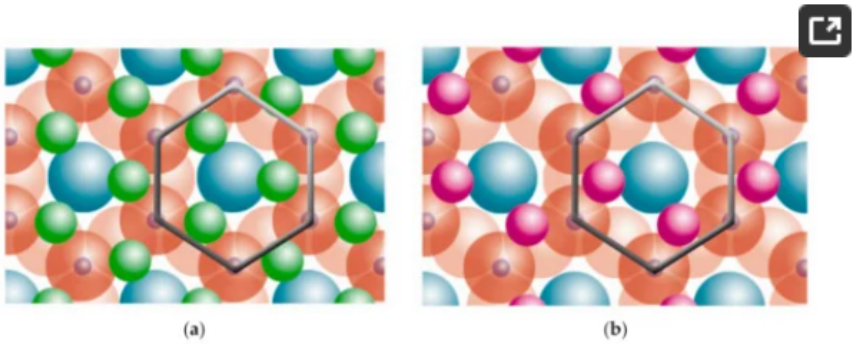


**Figure 6.** Schematic representation from the top view of the planes: (**a**) trioctahedral, (**b**) dioctahedral. oxygen, silicon, magnesium, aluminum, hydroxyl groups. Adapted from https://www.edafologia.net/, last visited 12 May 2021.

The octahedral $Mg^{2+}$ covers all positions in the trioctahedral plane (**Figure 6**a). However, the octahedral $Al^{3+}$ covers just two positions of three vacancies, and it is called the dioctahedral plane (**Figure 6**b). Nonetheless, this plane is within hexagonal networks.

The fifth plane corresponds to the superior plane of the octahedra (showed in **Figure 5**). If the structure ends in this plane, the clay has a T:O sequence (also known as 1:1 structure). However, if another tetrahedral layer is added, a sandwich-type T:O:T sequence is formed. The 1:1 sheet silicate is 7 Å thick, while the 2:1 sheet silicate is about 9 Å thick (**Figure 7**). Thus, the sheet silicates originate from the stacking of parallel planes with hexagonal symmetries, alternating the planes of ions (O and OH) and cations ($Si^{4+}$, $Al^{3+}$, and $Mg^{2+}$).

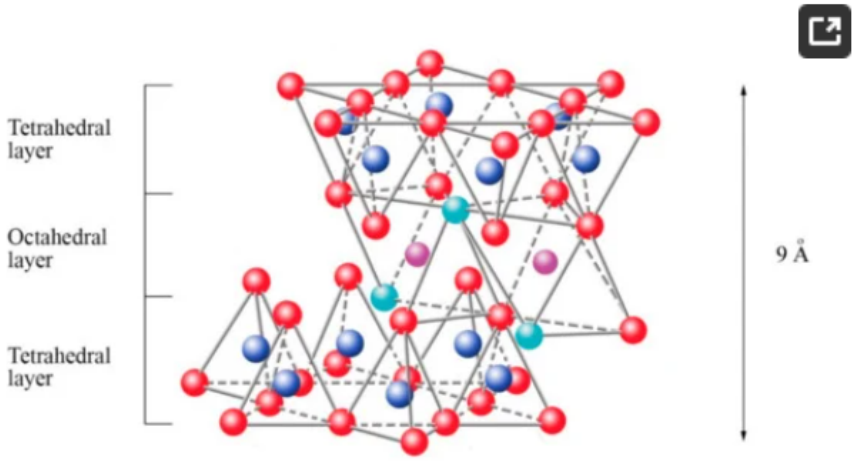


**Figure 7.** Schematic representation of the final structure corresponding to sheet 2:1. oxygen, silicon, magnesium/aluminum, hydroxyl groups. Adapted from https://www.edafologia.net/, last visited 12 May 2021.

Most sheet silicates are monoclinic or triclinic, and have several different polymorphs related to how T:O:T and T:O sheets stack to each other. **Figure 8** shows a representative diagram of the 1:1 and 2:1 sheet silicates to better visualize the structural arrangement described. **Table 1** shows the classification of clay minerals according to their structural configuration.

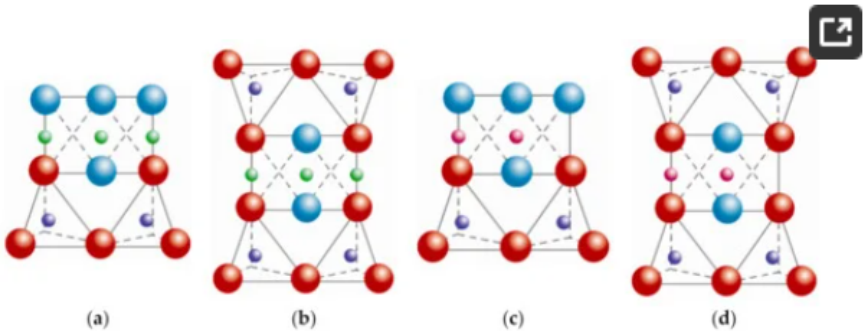


**Figure 8.** Schematic representation of the arrangement of the atomic planes: (**a**) 1:1 trioctahedral sheets, (**b**) 2:1 trioctahedral sheets, (**c**) 1:1 dioctahedral sheets, (**d**) 2:1 dioctahedral sheets. oxygen, silicon, magnesium/aluminum, hydroxyl groups. Adapted from https://www.edafologia.net/, last visited 12 May 2021.

**Table 1.** Classification of clay minerals.

| Structure | Dioctahedral | Trioctahedral |
|---|---|---|
| T:O | Kaolinite group [8][9][10][11][12][13][14][15][16][17][18][19][20][21][22][23][24] | Serpentine group [25][26][27] |
| | Pyrophyllite | Talc |

| Structure | Dioctahedral | Trioctahedral |
|---|---|---|
| T:O:T | Smectite group [28][29][30][31][32][33][34][35][36][37][38][39][40][41][42] | |
| | Montmorillonite [43][44][45][46][47][48][49][50][51][52][53][54][55][56][57][58][59][60][61][62][63][64][65][66][67][68][69][70][71][72][73][74][75] | Saponite |
| | Beidellite | Hectorite |
| | Nontronite | Stevensite |
| | Vermiculite group [12][76][77][78][79][80] | |
| | Illite | |
| | Mica group [79][81][82][83][84][85][86][87][88][89][90][91][92][93][94][95][96][97][98][99][100][101][102][103][104][105][106][107][108][109][110][111][112][113][114][115][116][117][118][119][120][121][122][123][124] | |
| | Muscovite | Biotite |
| | Paragonite | Phlogopite |
| | | Lepidolite |
| T:O:T:o | Chlorite group [125][126][127][128][129][130][131][132][133] | |
| | Paligorskite | Sepiolite |

Montmorillonite (discovered by Damour and Salvetat in Montmorillon, France) is currently the most widely used mineral clay to prepare polymer nanocomposites. It is a smectite-type clay belonging to the 2:1 sheet silicates and is composed of aluminosilicates ($Al^{3+}$). Montmorillonite clay has a high reaction capacity, exceptional resistance, and a large aspect ratio.

## 2. Cation Exchange Capacity

The ability to absorb a certain amount of cations and retain them in an exchangeable state is known as the cation exchange capacity (CEC), expressed in terms of milliequivalents per 100 g (meq/100 g) {Formatting Citation}. The charge of the layer is not locally constant as it varies from layer to layer and must instead be considered an average value over the whole crystal. The importance of knowing the CEC is that the sheets are not electrically neutral due to isomorphic substitutions, where others replace cations such as $Si^{4+}$ with a lower charge ($Al^{3+}$), promoting an excess of negative charge. In this case, the load balance is maintained by the presence of individual cations (as in the micas group) or hydrated cations (as in the case of vermiculites and smectites) in the interlaminar space, which is the existing space between two consecutive sheets, also known as "*galleries*" (**Figure 9**a). When the hydrated cations are ion-exchanged with organic cations such as more bulky alkylammonium, it usually results in a larger interlayer spacing.

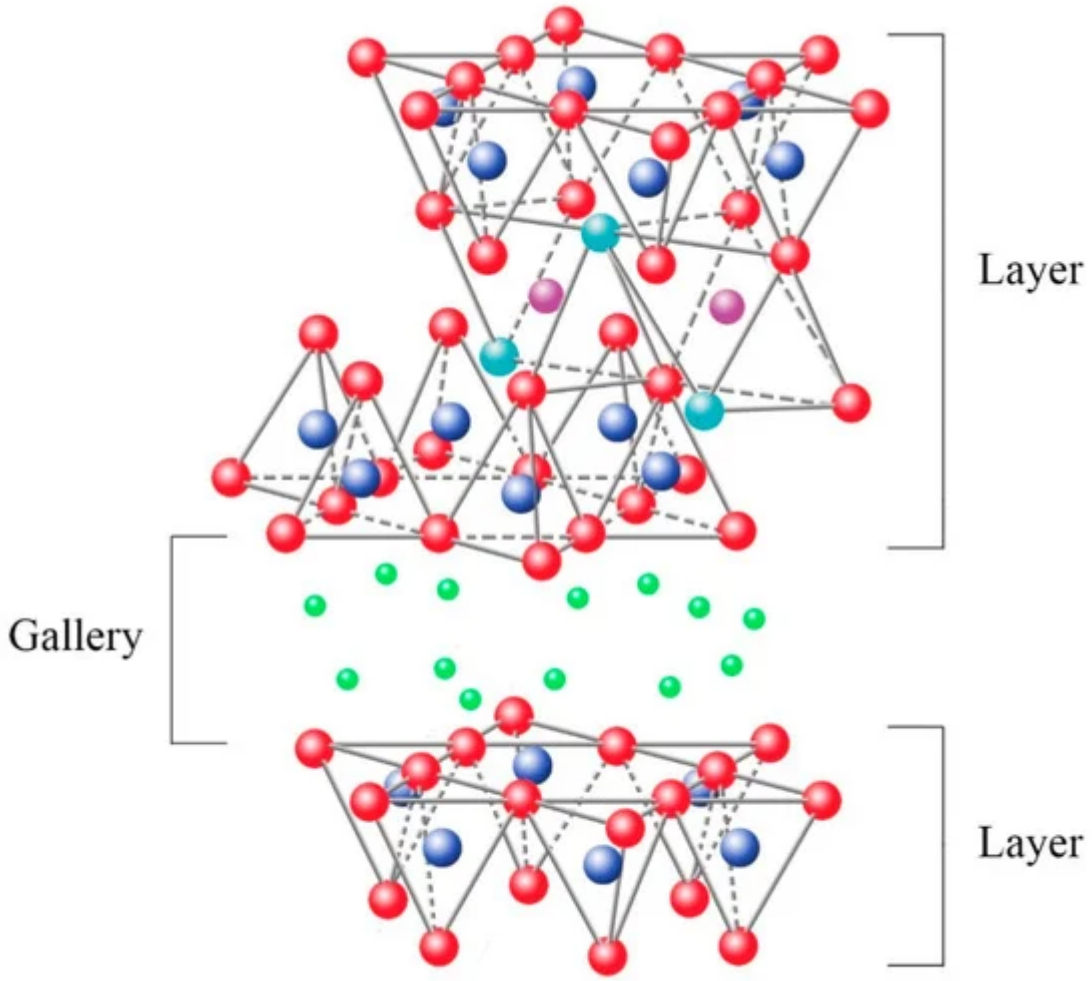


(a)

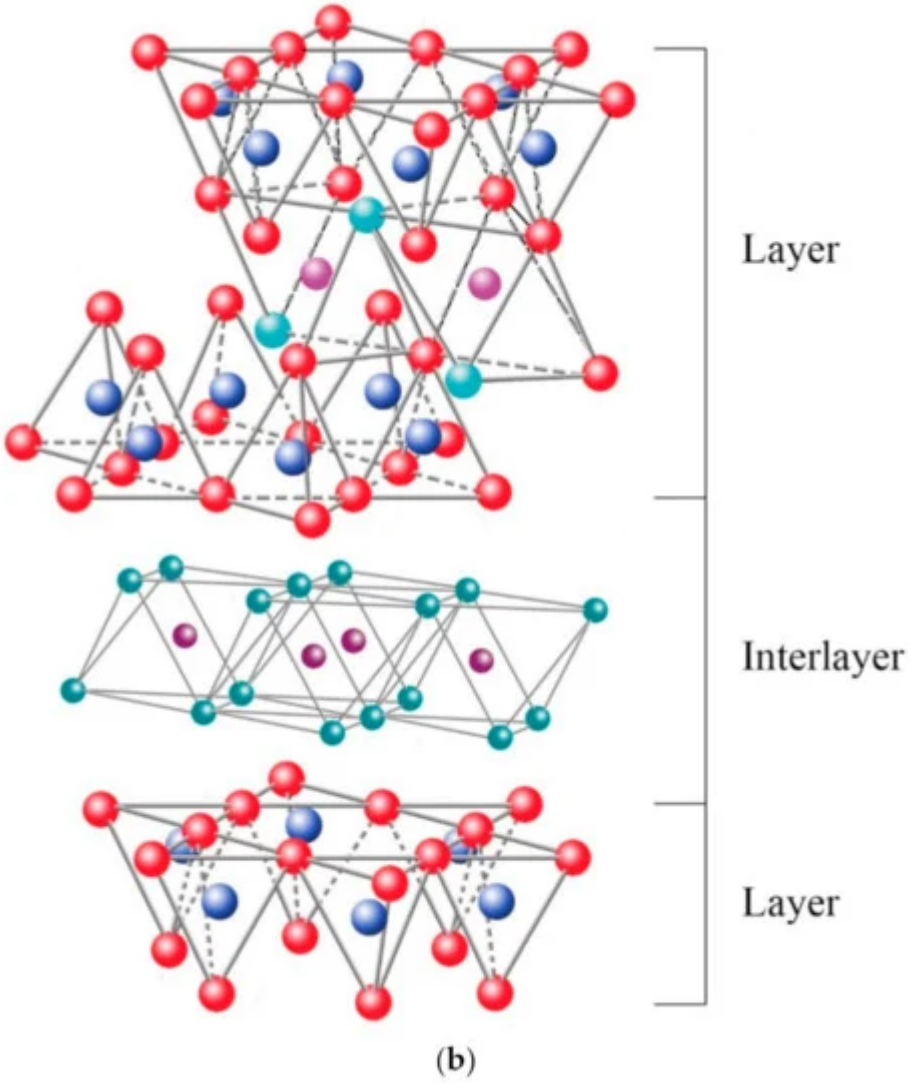


**Figure 9.** Schematic representation of the clay structure whose charge balance is maintained by: (**a**) interchange cations, (**b**) interlaminar octahedral layer. oxygen, silicon, magnesium/aluminum, hydroxyl groups. Schematic sketch based on Beyer [136] with permission from Elsevier.

Among the most frequent interlaminar cations are alkalines ($Na^+$ and $K^+$) and alkaline earth ($Mg^{2+}$). The hydrated cations such as water and different polar liquids increase the interlaminar space by swelling effect. If the interlaminar cations coordinate with OH groups, an octahedral layer would be formed within the interlaminar space (as chlorites, **Table 1**), developing structures T:O:T:o or 2:1:1, as represented in **Figure 9**b. In this case, the number 2 represents the two tetrahedral layers, while 1:1 indicates that the layers of the octahedra differ from each other since the interlaminar octahedra do not share vertices with the tetrahedra.

The bonding forces that join the sheets with the interlayer are weaker than those existing between the ions of the same sheet, so the phyllosilicates have a clear parallel direction of exfoliation.

## 3. Coupling Agents

In the first instance, clay minerals can only be miscible with hydrophilic polymers. Therefore, the use of coupling agents is necessary to make both phases compatible. These agents are fundamental molecules constituted by a hydrophilic functionality (related to clays) and by an organophilic functionality (related to the polymer), which favors the molecular compatibility between the sheets of the clay and the polymer chains.

The first coupled agents used to obtain nanocomposites were amino acids [134]. However, the most popular are alkylammonium ions, since they can easily be exchanged with the cations in the galleries. The alkylammonium ions are primary alkylamines [135][136]. Its basic formula is:

$$CH3−(CH2)n−NH3+ \quad (1)$$

where *n* represents the chain length, which ranges from 1 to 18 carbons. Lan et al. [137] highlighted that the exfoliation of the sheets is favored when ions with a chain length greater than eight carbon atoms are used, while with shorter chains, it led to the formation of agglomerated structures.

Ideally, the alkylammonium ions can be accommodated in various ways within the galleries, depending on the charge density of the clay minerals. Thus, the ions adopt monolayer, bilayer, or paraffin-like monolayers [138], as outlined in **Figure 10**.

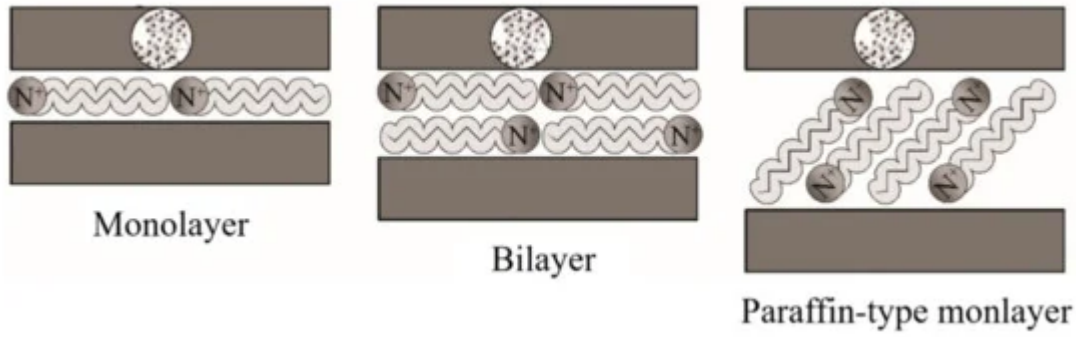


**Figure 10.** Schematic representation of the configuration of alkylammonium ions within the galleries of clays. Schematic figure based on Lagaly [139] with permission from Elsevier.

# 4. Nanocomposite Structures

Depending on the nature of the composite constituents (layered silicate, organic cation, and polymer matrix) and the method of preparation, three main types of composite may be obtained. Thus, polymer nanocomposites can be classified according to their morphology into agglomerates, intercalated, and exfoliated structures, as represented in **Figure 11**.

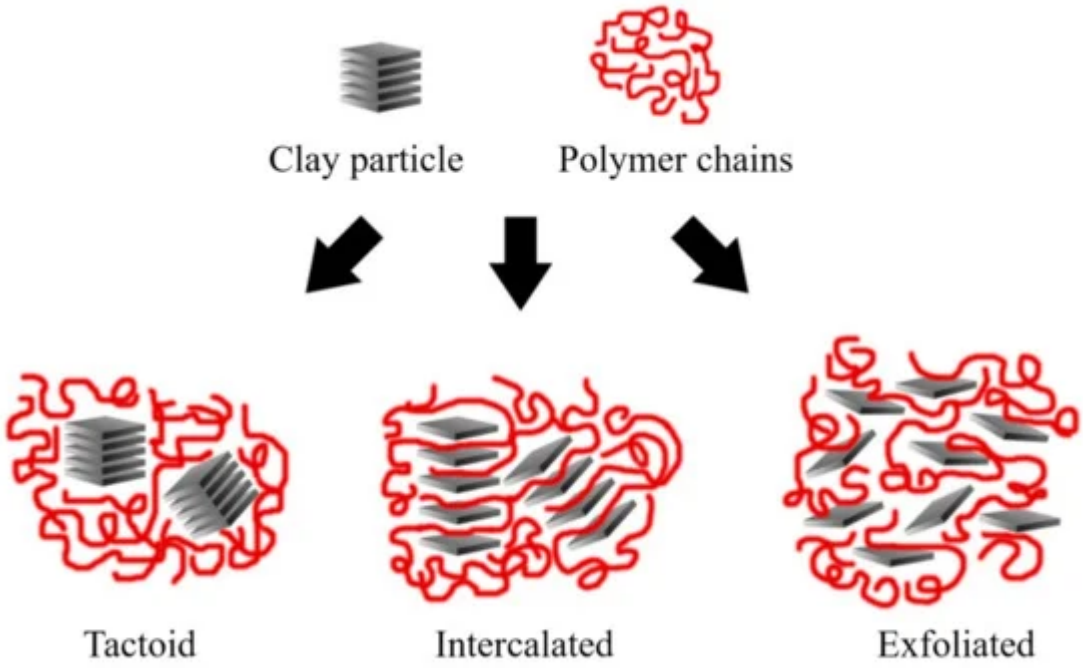


**Figure 11.** Schematic representation of the nanocomposite structures. Schematic figure based on Beyer [140] with permission from Elsevier.

Agglomerated composites are formed when the polymer is unable to intercalate between the sheets of clay. In this way, two separate and well-defined phases are obtained, where the sheets remain joined and aligned parallel to each other. It is common to classify the properties of these materials within the microcomposites. Some authors refer to the agglomerated composites as tactoids [1][138] or low-packing nanocomposites since there are no variations in the interlaminar space [1][5].

In the case of intercalated composites (also classified as flocculated [2]), the polymer chains are intercalated between the sheets of the clay, increasing the interlaminar space, obtaining a morphology of multiple highly ordered sheets.

Exfoliated nanocomposites contain sheets entirely separated and dispersed within the polymer matrix. This type of exfoliated structure presents relevant mechanical properties due to the high aspect ratio of single sheets. However, this structure is difficult to obtain, and three main processing strategies are commonly used.

## 5. Polymer Intercalation in Solution

The clay mineral is suspended in a polar organic solvent such as water, toluene, ethanol, etc., forming a gel-like structure. Subsequently, the polymer is dissolved and dispersed in the same type of solution, and the reaction is initiated by mixing the solutions, where polymer chains start to fill spaces in the galleries. Then, the solvent is removed by evaporation, obtaining the nanocomposite with a multilayered structure, as outlined in **Figure 12**.

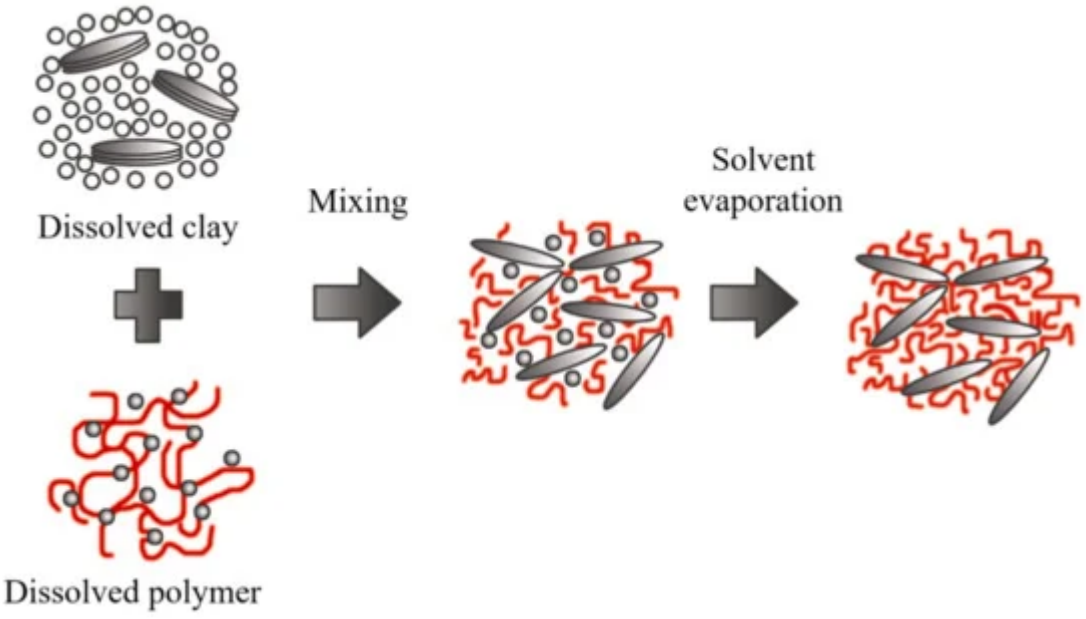


**Figure 12.** Schematic representation of polymer intercalation in solution. Schematic figure based on Zanetti [141] with permission from John Wiley and Sons, and Unalan [142] from RSC Adv. Open Access.

The nanocomposites obtained through this method are highly selective since the polymer and clay minerals possess different physical and chemical properties. The solvent is also essential because it is expensive and not environmentally friendly for large-scale production.

## 6. In Situ Polymerization

In this method, the galleries are expanded using a liquid monomer or a monomer in solution. The polymerization starts by the diffusion of an organic initiator or by catalysis through exchangeable cations (**Figure 13**) [143]. After polymerization termination, the solvent is evaporated, and the nanocomposite is ready for further modification. The in situ polymerization should be the best method to obtain high intermolecular distance between the clay layers. However, this method contains similar drawbacks to the solution-based method due to large-scale difficulties and environmental considerations.

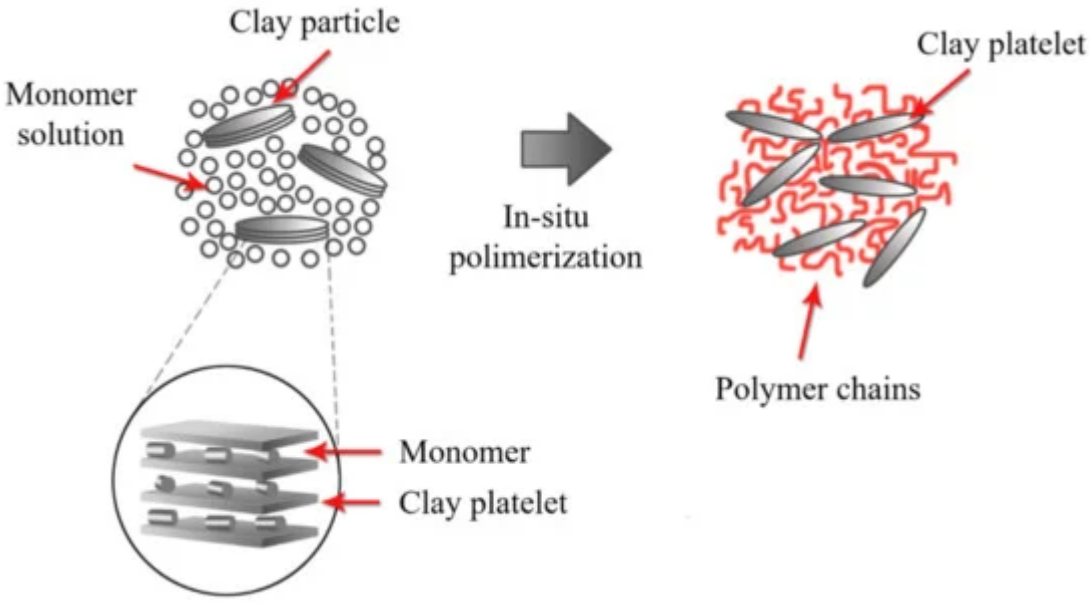


**Figure 13.** Schematic representation of in situ polymerization. Schematic figure based on Zanetti [141] with permission from John Wiley and Sons, and Unalan [142] from RSC Adv. Open Access.

## 7. Melt Blending Process

This method consists of mixing both phases (polymer and clay minerals) under the action of a high-temperature shear force. Melt intercalation is used for synthesizing thermoplastic polymer nanocomposites at a large scale. This procedure is compatible with industrial processes such as extrusion, making it more economical, convenient, and environmentally friendly because solvents are not required. However, the high temperatures during the extrusion process (up to 220 °C) can degrade the coupling agents (clay minerals modified with alkylammonium).

In a broad definition, the extrusion process refers to any transformation operation in which molten material is forced through a die to produce an article of constant cross-section and, in principle, indefinite length. In addition to plastics, many other materials are processed by extrusion, such as metals, ceramics, or food, obtaining very varied products such as aluminum or PVC window frames, pipes, pasta, etc. From a plastics point of view, extrusion is one of the essential transformation processes. The polymer is generally fed in solid form (commonly dust or pellet) in the hopper section and exits the extruder in the molten state. On some occasions, the polymer can be fed in molten form from a reactor where the extruder acts as a pump, providing the necessary pressure to pass the polymer through the nozzle. The extrusion process is frequently used to mix distinct materials, additives, and fillers to add better performance, reduce costs, and obtain multiple functionalities. These new formulations are further processed to create components or preforms using injection molding, blow molding, or thermoforming techniques.

Although there are various types of extruders, the most widely used are single-screw and twin-screw extruders. Specifically, a single-screw extruder can perform six main functions: transporting the solid material towards the melting zone, melting the polymer, pumping the melt, mixing, degassing, and forming. However, not all of the above functions necessarily take place during the operation of the extruder. According to the purpose, the extrusion

process starts with the material feeding system, a melting-plasticizing system, the pumping, and a pressurization system, generating a mixing effect.

It is common to find in the literature that single-screw extruders have poor material mixing due to their design. However, it is essential to consider many other factors that affect the end product, such as the wear of extruder working parts, rotational speed, pressure, nozzle type, and many more. In addition, the extruders are not just used for mixing but also for producing various materials, e.g., direct molding at the nozzle, injection into the die, etc. Ekielski et al. [144] evaluated the wear status of the single-screw extruder working elements based on die pressure and screw load values changes. The changes to these parameters were analyzed as a frequency spectrum using wavelet analysis tools. Due to the dynamic characteristics of the process in determining natural frequencies, the authors used the Morlet wavelet transform, observing that it is possible to accurately evaluate the degree of wear of the friction elements in a single-screw extruder.

Extrusion technology is also used in the food processing industry, known as extrusion-cooking, to produce so-called engineered foods and special feed. Leszek Moscicki and Dick J. van Zuilichem detailed an interesting work related to extrusion-cooking using single-screw extrusion technology [145]. The authors mentioned that the shear exerted by the rotating screw and the additional heating of the barrel promote a rheological modification. The physical aspects such as heat transfer, mass transfer, impulse transfer, residence time, and residence time distribution have a substantial impact on the properties of food and feed during extrusion-cooking and can drastically influence the quality of the final product.

Twin-screw extruders provide a much higher degree of shear than single-screw extruders, and the screw rotation can be co-rotating or counter-rotating. Therefore, this process can be too aggressive for some applications; even so, the high shear promotes twin-screw extrusion to prepare clay-based polymer nanocomposites (**Figure 14**). However, the single-screw extrusion should be considered for producing starch-based bionanocomposites or other natural composites.

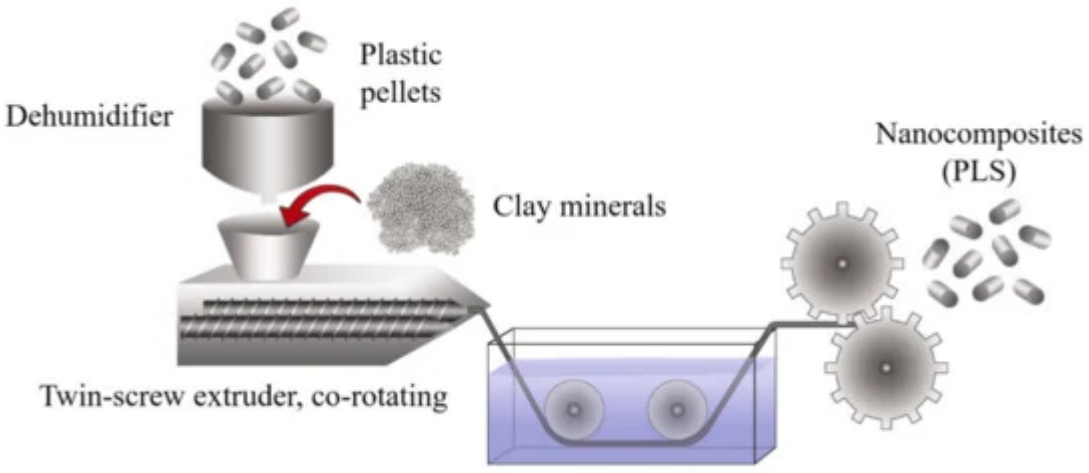


**Figure 14.** Schematic representation of the production process using twin-screw extrusion.

The literature is consistent in stating that the extrusion process leads to the development of intercalated structures. However, exfoliated structures can develop if there is high molecular compatibility between the phases, and in many instances, the use of additives is required (**Figure 15**).

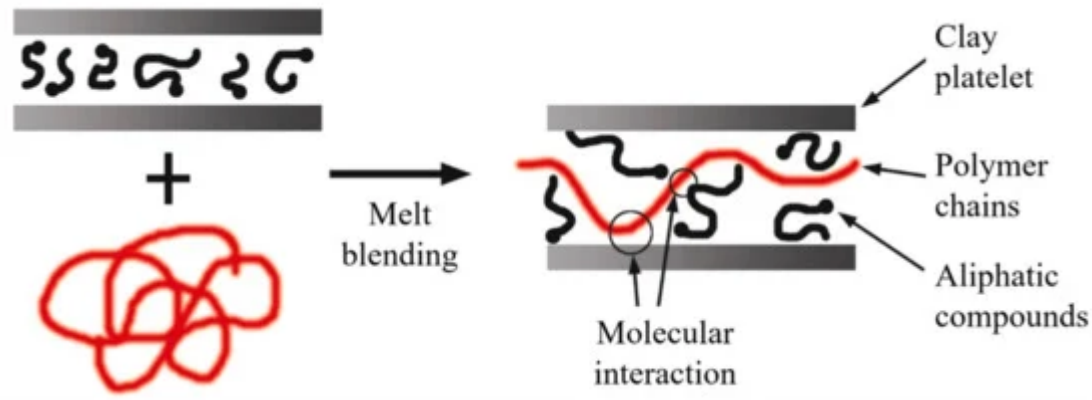


**Figure 15.** Schematic representation of intercalated structures for melt blending. Schematic figure based on Vaia [146] with permission from American Chemical Society, Copyright 1997.

Some authors [147][148][149] evaluated the influence of the extrusion process on the morphology of polymer nanocomposites. In this way, Dennis et al. [148] observed that a single screw extruder did not provide sufficient shear to separate or fracture the clay layers and did not offer an adequate residence time for layer dispersion. On the other hand, intercalated structures and some agglomerations are present when using a twin-screw extruder under the co-rotating configuration. By using the counter-rotating configuration, a high level of exfoliation was achieved.

Fornes et al. [149] found that the design of the extrusion screws also conditioned the morphology of the nanocomposites. The low- and medium-cut spindles developed interleaved structures, while a high-shear design obtained a high level of exfoliation.

Based on the previous studies, it is possible to consider that using a counter-rotating twin-screw extruder with high- or medium-shear screws should favor the exfoliation of the clay sheets. Nonetheless, it is important to consider that factors such as molecular compatibility and good processing conditions (dosage rate, temperature, and residence time, among others) are necessary for optimal exfoliation [150].

During the twin-screw extrusion process, the exfoliation mechanism begins with the fracture of the particles and the sliding of the sheets until they become stacked sheets of smaller size, as schematized in **Figure 16**a. This first phase requires a high shear intensity. Subsequently, the polymer is sandwiched between the sheets, taking advantage of their flexibility to increase the distance between them. This second phase requires both high shear and good molecular compatibility (**Figure 16**b). Finally, the exfoliated sheets are randomly dispersed within the matrix (**Figure 16**c), requiring adequate residence time [7][151].

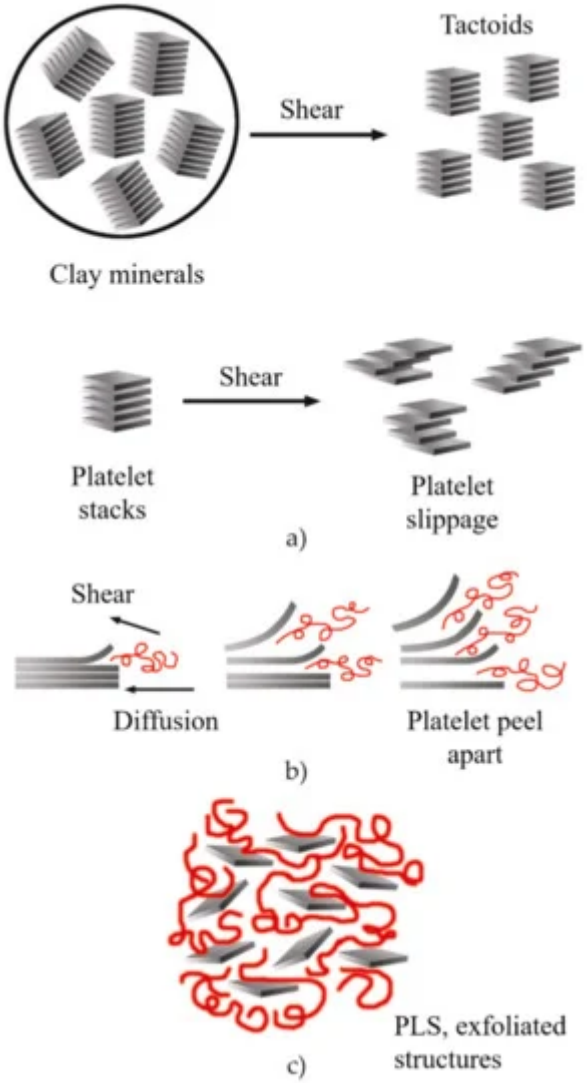


**Figure 16.** Schematic representation of the exfoliation mechanism of the clay platelets during the twin-screw extrusion process: (**a**) fracture and sliding of the sheets, (**b**) intercalation, (**c**) exfoliation. Schematic figure based on Fornes [152] with permission from Elsevier.

It is important to note that an intense shear does not guarantee a more significant number of exfoliated sheets. Similarly, a longer residence time does not provide better dispersion. For this reason, a large number of studies have focused on developing processing conditions that allow for increasing the level of exfoliation by using the melt intercalation process [153][4][7][149][151][154].

It is possible to consider the average dimensions of each particle: length ($\ell_p$), thickness ($t_p$), and aspect ratio ($\ell_p/t_p$). Some authors [7] detailed that the increase in $\ell_p$ can be related to the sliding of the sheets that occurred during the twin-screw extrusion process, which can be defined as effective particle length, as shown in **Figure 17**.

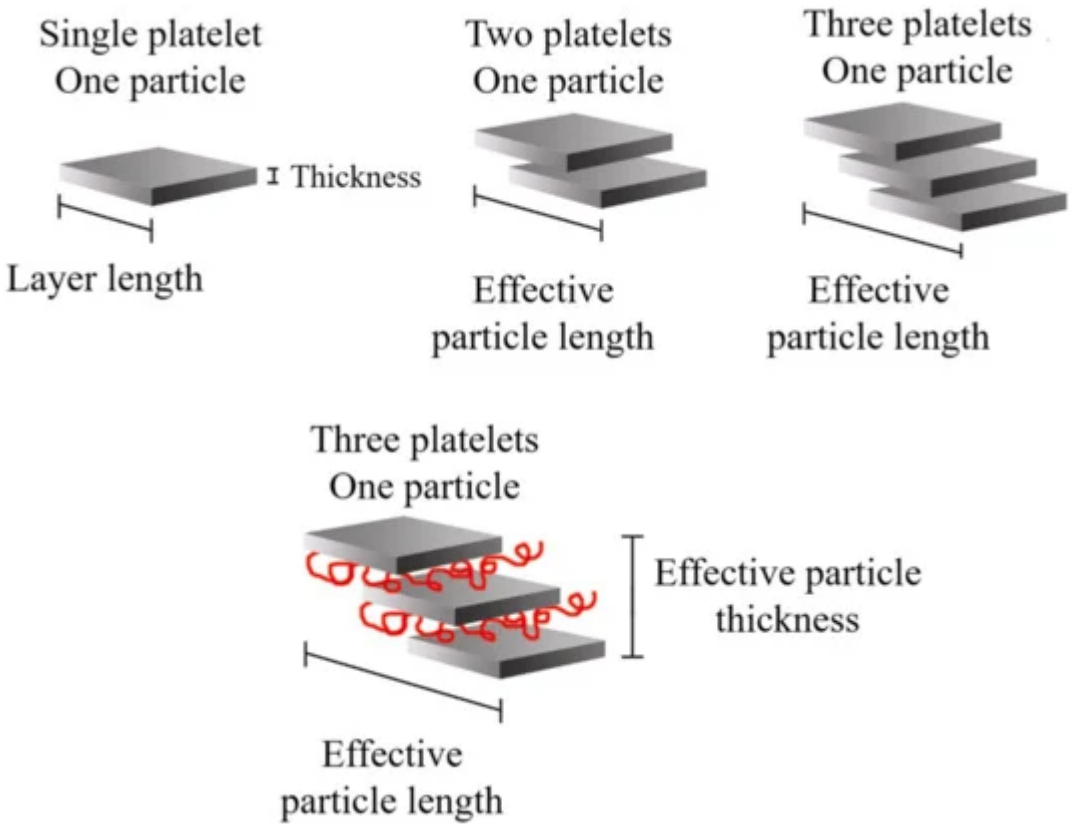


**Figure 17.** Schematic representation of the effective length and thickness of the clay particles present in nanocomposites with a certain degree of intercalation. Schematic figure based on Fornes [152] and Chavarria [155] with permission from Elsevier.

The clay-based polymer nanocomposites have gained the attention of academics and industry in recent decades. Integrating small percentages of clay minerals into the polymer matrix improves the mechanical properties compared to neat polymers. Properly dispersed and aligned clay platelets have proven to be very effective for increasing stiffness without altering the polymer density. There is extensive literature regarding the mechanical properties of polymers enhanced by low clay content, as summarized in **Table 2**.

**Table 2.** Mechanical properties for clay-based polymer nanocomposites.

| Mechanical Test | References |
|---|---|
| Tensile | [2][156][157][158][159][160][161][162][163][164][165][166][167][168][169][170][171][172][173][174][175][176][177][178][179][180][181][182][183][184][185][186] |
| Compression | [163][180] |
| Bending | [187][188][189][190][191][192] |

## References

1. Alexandre, M.; Dubois, P. Polymer-layered silicate nanocomposites: Preparation, properties and uses of a new class of materials. Mater. Sci. Eng. R Rep. 2000, 28, 1–63.
2. Sinha Ray, S.; Okamoto, M. Polymer/layered silicate nanocomposites: A review from preparation to processing. Prog. Polym. Sci. 2003, 28, 1539–1641.
3. Minerals, S.; Page, I.; The, S.M.; Guggenheim, S.; Martin, R.T.; Alietti, A.; Drits, V.A.; Formoso, M.L.L.; Galán, E.; Köster, H.M.; et al. Clays, nanoclays, and montmorillonite minerals. Dev. Clay Sci. 2017, 148, 255–256.
4. Camargo, P.H.C.; Satyanarayana, K.G.; Wypych, F. Nanocomposites: Synthesis, structure, properties and new application opportunities. Mater. Res. 2009, 12, 1–39.
5. Giannelis, E.P. Polymer layered silicate nanocomposites. Adv. Mater. 1996, 8, 29–35.
6. Hanemann, T.; Szabó, D.V. Polymer-Nanoparticle Composites: From Synthesis to Modern Applications. Materials 2010, 3, 3468–3517.
7. Paul, D.R.; Robeson, L.M. Polymer nanotechnology: Nanocomposites. Polymer 2008, 49, 3187–3204.
8. Papp, S.; Szucs, A.; Dékány, I. Colloid synthesis of monodisperse Pd nanoparticles in layered silicates. Solid State Ion. 2001, 141–142, 17169–17211.
9. Papp, S.; Szel, J.; Dékány, I. Stabilization of rhodium nanoparticles in an aqueous medium by polymer and layered silicates. Nanotechnology 2003, 5118, 646–656.
10. Ruiz-Hitzky, E.; Aranda, P.; Darder, M. Hybrid and Biohybrid Materials Based on Layered Clays. In Tailored Organic-Inorganic Materials; John Wiley & Sons, Inc.: Hoboken, NJ, USA, 2015; pp. 245–297. ISBN 9781118792223.
11. Ouchiar, S.; Stoclet, G.; Cabaret, C.; Georges, E.; Smith, A.; Martias, C.; Addad, A.; Gloaguen, V. Comparison of the influence of talc and kaolinite as inorganic fillers on morphology, structure and thermomechanical properties of polylactide based composites. Appl. Clay Sci. 2015, 116–117.
12. Sleptsova, S.A.; Okhlopkova, A.A.; Kapitonova, I.V.; Lazareva, N.N.; Makarov, M.M.; Nikiforov, L.A. Spectroscopic study of tribooxidation processes in modified PTFE. J. Frict. Wear 2016, 37.
13. Iqbal, S.; Inam, F.; Iqbal, N.; Jamil, T.; Bashir, A.; Shahid, M. Thermogravimetric, differential scanning calorimetric, and experimental thermal transport study of functionalized nanokaolinite-doped elastomeric nanocomposites. J. Therm. Anal. Calorim. 2016, 125.
14. Malkappa, K.; Rao, B.N.; Jana, T. Functionalized polybutadiene diol based hydrophobic, water dispersible polyurethane nanocomposites: Role of organo-clay structure. Polymer 2016, 99.
15. Neto, J.C.M.; Kimura, S.P.R.; Adeodato, M.G.; Neto, J.E.; Do Nascimento, N.R.; Lona, L.M.F. Intercalation and exfoliation mechanism of kaolinite during the emulsion polymerization. Chem.

Eng. Trans. 2017, 57.

16. Youssef, A.M.; El-Sayed, S.M. Bionanocomposites materials for food packaging applications: Concepts and future outlook. Carbohydr. Polym. 2018, 193.
17. Cabedo, L.; Plackett, D.; Giménez, E.; Lagarón, J.M. Studying the degradation of polyhydroxybutyrate-co-valerate during processing with clay-based nanofillers. J. Appl. Polym. Sci. 2009, 112.
18. Letaief, S.; Christian, D. Functionalization of the interlayer surfaces of kaolinite by alkylammonium groups from ionic liquids. Clays Clay Miner. 2009, 57.
19. Sun, D.; Li, Y.; Zhang, B.; Pan, X. Preparation and characterization of novel nanocomposites based on polyacrylonitrile/kaolinite. Compos. Sci. Technol. 2010, 70.
20. Rhim, J.W.; Park, H.M.; Ha, C.S. Bio-nanocomposites for food packaging applications. Prog. Polym. Sci. 2013, 38.
21. Weiss, S.; Hirsemann, D.; Biersack, B.; Ziadeh, M.; Müller, A.H.E.; Breu, J. Hybrid Janus particles based on polymer-modified kaolinite. Polymer 2013, 54.
22. Kirillina, I.V.; Nikiforov, L.A.; Okhlopkova, A.A.; Sleptsova, S.A.; Yoon, C.; Cho, J.H. Nanocomposites based on polytetrafluoroethylene and ultrahigh molecular weight polyethylene: A brief review. Bull. Korean Chem. Soc. 2014, 35.
23. Cui, Y.; Kumar, S.; Rao Kona, B.; Van Houcke, D. Gas barrier properties of polymer/clay nanocomposites. RSC Adv. 2015, 5.
24. Poikelispää, M.; Das, A.; Dierkes, W.; Vuorinen, J. The effect of coupling agents on silicate-based nanofillers/carbon black dual filler systems on the properties of a natural rubber/butadiene rubber compound. J. Elastomers Plast. 2015, 47.
25. Dang, W.; Lorenzelli, L.; Vinciguerra, V.; Dahiya, R. Hybrid structure of stretchable interconnect for reliable E-skin application. In Proceedings of the IEEE International Symposium on Industrial Electronics, Edinburgh, UK, 19–21 June 2017.
26. Dolgopolov, K.N.; Lyubimov, D.N. Evaluation of tribological properties of components of polymer composite selflubricating materials. MATEC Web Conf. 2018, 226, 01005.
27. Valentin, T.M.; Dubois, E.M.; Machnicki, C.E.; Bhaskar, D.; Cui, F.R.; Wong, I.Y. 3D printed self-adhesive PEGDA-PAA hydrogels as modular components for soft actuators and microfluidics. Polym. Chem. 2019, 10.
28. Kotsilkova, R.; Petkova, V.; Pelovski, Y. Thermal analysis of polymer-silicate nanocomposites. J. Therm. Anal. Calorim. 2001, 64, 591–598.

29. Kotsilkova, R. Rheology-structure relationship of polymer/layered silicate hybrids. Mech. Time-Depend. Mater. 2002, 6.
30. Kiersnowski, A.; Serwadczak, M.; Kułaga, E.; Futoma-Kołoch, B.; Bugla-Płoskońska, G.; Kwiatkowski, R.; Doroszkiewicz, W.; Pigłowski, J. Delamination of montmorillonite in serum-A new approach to obtaining clay-based biofunctional hybrid materials. Appl. Clay Sci. 2009, 44.
31. Szczerba, M.; Środoń, J.; Skiba, M.; Derkowski, A. One-dimensional structure of exfoliated polymer-layered silicate nanocomposites: A polyvinylpyrrolidone (PVP) case study. Appl. Clay Sci. 2010, 47.
32. Lan, Y.F.; Lee, R.H.; Lin, J.J. Aqueous dispersion of conjugated polymers by colloidal clays and their film photoluminescence. J. Phys. Chem. B 2010, 114.
33. Tamura, K.; Yamada, H. Morphology Generation in Polymer Nanocomposites Using Various Layered Silicates. Optim. Polym. Nanocomposite Prop. 2010, 198.
34. Pascua, C.S.; Ohnuma, M.; Matsushita, Y.; Tamura, K.; Yamada, H.; Cuadros, J.; Ye, J. Synthesis of monodisperse Zn-smectite. Appl. Clay Sci. 2010, 48.
35. Chang, Y.C.; Chou, C.C.; Lin, J.J. Emulsion intercalation of smectite clays with comb-branched copolymers consisting of multiple quaternary amine salts and a poly(styrene-butadiene- styrene) backbone. Langmuir 2005, 21.
36. Dudkina, M.M.; Tenkovtsev, A.V.; Pospiech, D.; Jehnichen, D.; Häußler, L.; Leuteritz, A. Nanocomposites of NLO chromophore-modified layered silicates and polypropylene. J. Polym. Sci. Part B Polym. Phys. 2005, 43.
37. Leroux, F. Organo-modified anionic clays into polymer compared to smectite-type nanofiller: Potential applications of the nanocomposites. J. Nanosci. Nanotechnol. 2006, 6.
38. Wang, H.W.; Dong, R.X.; Liu, C.L.; Chang, H.Y. Effect of clay on properties of polyimide-clay nanocomposites. J. Appl. Polym. Sci. 2007, 104.
39. Liu, T.; Chen, B.; Evans, J.R.G. Ordered assemblies of clay nano-platelets. Bioinspir. Biomim. 2008, 3.
40. Darder, M.; Aranda, P.; Ruiz, A.I.; Fernandes, F.M.; Ruiz-Hitzky, E. Design and preparation of bionanocomposites based on layered solids with functional and structural properties. Mater. Sci. Technol. 2008, 24, 1100–1110.
41. Watanabe, H.; Matsushima, H.; Fuji, M.; Takahashi, M. Electrophoretic Deposition of Smectite Particles onto Cupper Plate. Key Eng. Mater. 2009, 412, 195–200.
42. Maiti, M.; Bhowmick, A.K. Synthesis and properties of new fluoroelastomer nanocomposites from tailored anionic layered magnesium silicates (hectorite). J. Appl. Polym. Sci. 2009, 111.

43. Suh, D.J.; Park, O.O.; Mun, J.; Yoon, C.S. Photorefractive behaviors in a polymer composite including layered silicates. Appl. Clay Sci. 2002, 21.
44. Wang, K.; Liang, S.; Du, R.; Zhang, Q.; Fu, Q. The interplay of thermodynamics and shear on the dispersion of polymer nanocomposite. Polymer 2004, 45.
45. Shi, X.; Gan, Z. Preparation and characterization of poly(propylene carbonate)/montmorillonite nanocomposites by solution intercalation. Eur. Polym. J. 2007, 43.
46. Dornelas, C.B.; Resende, D.K.; Tavares, M.I.B.; Gomes, A.S.; Cabral, L.M. Preparation and reactional evaluation of formation of PVP K-30 - Montmorillonite (natural and organophilic) by X ray diffraction. Polímeros 2008, 18.
47. Wang, C.A.; Long, B.; Lin, W.; Huang, Y.; Sun, J. Poly(amic acid)-clay nacrelike composites prepared by electrophoretic deposition. J. Mater. Res. 2008, 23.
48. Galimberti, M.; Martino, M.; Guenzi, M.; Leonardi, G.; Citterio, A. Thermal stability of ammonium salts as compatibilizers in polymer/layered silicate nanocomposites. E-Polymers 2009.
49. Buruiana, T.; Melinte, V.; Buruiana, E.C.; Mihai, A. Synthesis and characterization of polyurethane cationomer/MMT hybrid composite. Polym. Int. 2009, 58.
50. Gao, J.; Guo, N.; Liu, Y.; Li, J.; Hu, H.; Sun, L.; Zhang, X. Effect of compound technology on polyethylene/montmorillonite composites. In Proceedings of the IEEE International Conference on Properties and Applications of Dielectric Materials, Harbin, China, 19–23 July 2009.
51. Soundararajah, Q.Y.; Karunaratne, B.S.B.; Rajapakse, R.M.G. Mechanical properties of poly(vinyl alcohol) montmorillonite nanocomposites. J. Compos. Mater. 2010, 44.
52. Chang, M.K.; Hsieh, H.H.; Li, S.J. A Study of Thermal Stability and Electromaganetic Shielding Behavior of Polyaniline-P-Toluene Sulfonic Acid/Montmorillonite Nanocomposites. Appl. Mech. Mater. 2011, 52–54, 180–185.
53. Monsiváis-Barrón, A.J.; Bonilla-Rios, J.; Ramos De Valle, L.F.; Palacios, E. Oxygen permeation properties of HDPE-layered silicate nanocomposites. Polym. Bull. 2013, 70.
54. Shiravand, F.; Hutchinson, J.M.; Calventus, Y. Influence of the isothermal cure temperature on the nanostructure and thermal properties of an epoxy layered silicate nanocomposite. Polym. Eng. Sci. 2014, 54.
55. Wooster, T.J.; Abrol, S.; MacFarlane, D.R. Cyanate ester polymerization catalysis by layered-silicates. Polymer 2004, 45.
56. Jin, X.; Hu, X.; Wang, Q.; Wang, K.; Yao, Q.; Tang, G.; Chu, P.K. Multifunctional cationic polymer decorated and drug intercalated layered silicate (NLS) for early gastric cancer prevention. Biomaterials 2014, 35.

57. Riaz, U.; Ashraf, S.M.; Verma, A. Influence of Conducting Polymer as Filler and Matrix on the Spectral, Morphological and Fluorescent Properties of Sonochemically Intercalated poly(o-phenylenediamine)/Montmorillonite Nanocomposites. Recent Pat. Nanotechnol. 2016, 10.
58. Ghosh, S.K.; Rahman, W.; Middya, T.R.; Sen, S.; Mandal, D. Improved breakdown strength and electrical energy storage performance of γ-poly(vinylidene fluoride)/unmodified montmorillonite clay nano-dielectrics. Nanotechnology 2016, 27.
59. Pu, W.F.; Yang, Y.; Yuan, C.D. Gelation performance of poly(ethylene imine) crosslinking polymer–layered silicate nanocomposite gel system for potential water-shutoff use in high-temperature reservoirs. J. Appl. Polym. Sci. 2016, 133.
60. Saldābola, R.; Merijs Meri, R.; Zicans, J.; Ivanova, T.; Berzina, R. PC/ABS Nanocomposites with Layered Silicates Obtaining, Structure and Properties. Key Eng. Mater. 2016, 721, 38–42.
61. Hernandez-Guerrero, O.; Castillo-Pérez, R.; Hernández-Vargas, M.L.; Campillo-Illanes, B.F. Study of Thermal and Mechanical Properties of Clay/Polymer Nanocomposite Synthesized Via Modified Solution Blending. MRS Adv. 2017, 2, 2757–2762.
62. El-Sheikhy, R.; Al-Shamrani, M. Interfacial bond assessment of clay-polyolefin nanocomposites CPNC on view of mechanical and fracture properties. Adv. Powder Technol. 2017, 28.
63. İlk, S.; Şener, M.; Vural, M.; Serçe, S. Chitosan/Octadecylamine-Montmorillonite Nanocomposite Containing Nigella arvensis Extract as Improved Antimicrobial Biofilm Against Foodborne Pathogens. Bionanoscience 2018, 8.
64. Ashok Gandhi, R.; Jayaseelan, V.; Raghunath, B.K.; Palanikumar, K.; Ramachandran, S. Nano indendation hardness testing of PP-CNT composites. Mater. Today Proc. 2019, 16, 1372–1377.
65. Shuai, C.; Li, Y.; Feng, P.; Yang, W.; Zhao, Z.; Liu, W. Montmorillonite reduces crystallinity of poly-l-lactic acid scaffolds to accelerate degradation. Polym. Adv. Technol. 2019, 30.
66. Chou, C.C.; Lin, J.J. One-step exfoliation of montmorillonite via phase inversion of amphiphilic copolymer emulsion. Macromolecules 2005, 38.
67. Attia, N.F.; Nour, M.; Hassan, M.; Mohamed, G.; Oh, H.; Mahmoud, M. Effect of type of organic modifier on the clay layered-based nanocomposites flammability and toxic gases emission. J. Thermoplast. Compos. Mater. 2020.
68. Zubair, M.; Ullah, A. Recent advances in protein derived bionanocomposites for food packaging applications. Crit. Rev. Food Sci. Nutr. 2020, 60.
69. Meng, N.; Zhang, M.; Ge, M.Q.; Zhou, N.; Chi, C.; Chu, X.; Sun, B.; Gao, X. Montmorillonite-lecithin-heparin/PDMS films with enhanced mechanical and antithrombogenic properties. Polym. Compos. 2020, 41.

70. Sheu, Z.; Cheng, Y.B.; Simon, G.P. Sequential and simultaneous melt intercalation of poly(ethylene oxide) and poly(methyl methacrylate) into layered silicates. Macromolecules 2005, 38.
71. Qin, H.; Zhang, S.; Liu, H.; Xie, S.; Yang, M.; Shen, D. Photo-oxidative degradation of polypropylene/montmorillonite nanocomposites. Polymer 2005, 46.
72. Rehab, A.; Salahuddin, N. Nanocomposite materials based on polyurethane intercalated into montmorillonite clay. Mater. Sci. Eng. A 2005, 399.
73. Hao, X.; Gai, G.; Liu, J.; Yang, Y.; Zhang, Y.; Nan, C.W. Flame retardancy and antidripping effect of OMT/PA nanocomposites. Mater. Chem. Phys. 2006, 96.
74. Zhu, Y.; Wang, B.; Gong, W.; Kong, L.; Jia, Q. Investigation of the hydrogen-bonding structure and miscibility for PU/EP IPN nanecomposites by PALS. Macromolecules 2006, 39.
75. Román, F.; Montserrat, S.; Hutchinson, J.M. On the effect of montmorillonite in the curing reaction of epoxy nanocomposites. J. Therm. Anal. Calorim. 2007, 87, 113–118.
76. Vasilev, A.P.; Struchkova, T.S.; Nikiforov, L.A.; Okhlopkova, A.A.; Grakovich, P.N.; Shim, E.L.; Cho, J.H. Mechanical and tribological properties of polytetrafluoroethylene composites with carbon fiber and layered silicate fillers. Molecules 2019, 24, 224.
77. Wan, Y.; Fan, Y.; Dan, J.; Hong, C.; Yang, S.; Yu, F. A review of recent advances in two-dimensional natural clay vermiculite-based nanomaterials. Mater. Res. Express 2019, 6.
78. Leont’ev, L.B.; Shapkin, N.P.; Leont’ev, A.L. Effect of the Chemical Composition and Structural Characteristics of Vermiculite-Based Tribotechnical Materials on the Operating Ability of the Coatings Formed. J. Mach. Manuf. Reliab. 2020, 49.
79. Mittal, V. High CEC generation and surface modification in mica and vermiculite minerals. Philos. Mag. 2013, 93.
80. Sleptsova, S.A.; Afanas’eva, E.S.; Grigor’eva, V.P. Structure and tribological behavior of polytetrafluoroethylene modified with layered silicates. J. Frict. Wear 2009, 30.
81. Mehrotra, V.; Giannelis, E.P. Metal-insulator molecular multilayers of electroactive polymers: Intercalation of polyaniline in mica-type layered silicates. Solid State Commun. 1991, 77.
82. Gaylarde, P.; Gaylarde, C. Deterioration of siliceous stone monuments in Latin America: Microorganisms and mechanisms. Corros. Rev. 2004, 22.
83. Heinz, H.; Koerner, H.; Anderson, K.L.; Vaia, R.A.; Farmer, B.L. Force field for mica-type silicates and dynamics of octadecylammonium chains grafted to montmorillonite. Chem. Mater. 2005, 17.
84. Zhang, X.; Lin, G.; Abou-Hussein, R.; Hassan, M.K.; Noda, I.; Mark, J.E. Some novel layered-silicate nanocomposites based on a biodegradable hydroxybutyrate copolymer. Eur. Polym. J.

2007, 43.

85. Zhang, Y.H.; Su, Q.S.; Yu, L.; Liao, L.B.; Zheng, H.; Huang, H.T.; Zhang, G.G.; Yao, Y.B.; Lau, C.; Chan, H.L.W. Preparation of Low-K Fluorinated Polyimide/Phlogopite Nanocomposites. Adv. Mater. Res. 2008, 47–50, 987–990.
86. Bae, S.H.; Yoo, S.I.; Bae, W.K.; Lee, S.; Lee, J.K.; Sohn, B.H. Single-layered films of diblock copolymer micelles containing quantum dots and fluorescent dyes and their fluorescence resonance energy transfer. Chem. Mater. 2008, 20.
87. Miwa, Y.; Drews, A.R.; Schlick, S. Unique structure and dynamics of poly(ethylene oxide) in layered silicate nanocomposites: Accelerated segmental mobility revealed by simulating ESR spectra of spin-labels, XRD, FTIR, and DSC. Macromolecules 2008, 41.
88. Fujii, K.; Ishihama, Y.; Sakuragi, T.; Ohshima, M.A.; Kurokawa, H.; Miura, H. Heterogeneous catalysts immobilizing α-diimine nickel complexes into fluorotetrasilicic mica interlayers to prepare branched polyethylene from only ethylene. Catal. Commun. 2008, 10.
89. Pacheco-Torgal, F.; Castro-Gomes, J.; Jalali, S. Tungsten mine waste geopolymeric binder: Preliminary hydration products investigations. Constr. Build. Mater. 2009, 23.
90. Cheng, H.Y.; Jiang, G.J.; Hung, J.Y. Enhanced mechanical and thermal properties of PS/mica and PMMA/mica nanocomposites by emulsion polymerization. Polym. Compos. 2009, 30.
91. Tamura, K.; Uno, H.; Yamada, H.; Umeyama, K. Layered silicate-polyamide-6 nanocomposites: Influence of silicate species on morphology and properties. J. Polym. Sci. Part B Polym. Phys. 2009, 47.
92. Herzog, E.; Caseri, W.; Suter, U.W. Adsorption of polymers with crown ether substituents on muscovite mica. Colloid Polym. Sci. 1994, 272.
93. Möller, M.W.; Handge, U.A.; Kunz, D.A.; Lunkenbein, T.; Altstädt, V.; Breu, J. Tailoring shear-stiff, mica-like nanoplatelets. ICS Nano 2010, 4, 717–724.
94. Lin, J.J.; Chan, Y.N.; Lan, Y.F. Hydrophobic modification of layered clays and compatibility for epoxy nanocomposites. Materials 2010, 3, 2588–2605.
95. Manias, E.; Heidecker, M.J.; Nakajima, H.; Costache, M.C.; Wilkie, C.A. Poly(ethylene terephthalate) nanocomposites using nanoclays modified with thermally stable surfactants. Therm. Stable Flame Retard. Polym. Nanocompos. 2011, 9780521190, 100.
96. Schütz, M.R.; Kalo, H.; Lunkenbein, T.; Gröschel, A.H.; Müller, A.H.E.; Wilkie, C.A.; Breu, J. Shear stiff, surface modified, mica-like nanoplatelets: A novel filler for polymer nanocomposites. J. Mater. Chem. 2011, 21.
97. Fu, Y.T.; Zartman, G.D.; Yoonessi, M.; Drummy, L.F.; Heinz, H. Bending of layered silicates on the nanometer scale: Mechanism, stored energy, and curvature limits. J. Phys. Chem. C 2011, 115.

98. Ahmad Rasyid, M.F.; Hazizan, M.A.; Sharif, J.M. Influence of Organo-Clay on Mechanical and Thermal Properties of O-Muscovite/PP Layered Silicate Nanocomposite. Adv. Mater. Res. 2011, 364, 174–180.
99. Xu, X.; Ding, H.; Wang, Y.B.; Liang, Y.; Jiang, W. Preparation and Characterization of Activated Sericite Modified by Fluorosilicate. Adv. Mater. Res. 2012, 427, 70–76.
100. Wang, X.Y.; Liu, B.; Tang, Y.F.; Su, H.J.; Han, Y.; Sun, R.C. New progress on rectorite/polymer nanocomposites. Wuji Cailiao Xuebao J. Inorg. Mater. 2012, 27.
101. Kudus, M.H.A.; Akil, H.M.; Rasyid, M.F.A. Muscovite-MWCNT hybrid as a potential filler for layered silicate nanocomposite. Mater. Lett. 2012, 79.
102. Mittal, V. Surface modification of layered silicates. II. Factors affecting thermal stability. Philos. Mag. 2012, 92.
103. Olson, B.G.; Peng, Z.L.; Srithawatpong, R.; McGervey, J.D.; Ishida, H.; Jamieson, A.M.; Manias, E.; Giannelis, E.P. Free volume in layered organosilicate-polystyrene nanocomposites. Mater. Sci. Forum 1997, 255–257.
104. Livi, S.; Duchet-Rumeau, J.; Gérard, J.F. Effect of ionic liquid modified synthetic layered silicates on thermal and mechanical properties of high density polyethylene nanocomposites. Macromol. Symp. 2014, 342.
105. Omar, M.F.; Abd Wahab, N.S.; Akil, H.M.; Ahmad, Z.A.; Rasyid, M.F.A.; Noriman, N.Z. Effect of Surface Modification on Strain Rate Sensitivity of Polypropylene/Muscovite Layered Silicate Composites. Mater. Sci. Forum 2014, 803, 343–347.
106. Omar, M.F.; Jaya, H.; Akil, H.M.; Ahmad, Z.A.; Rasyid, M.F.A.; Noriman, N.Z. Effect of Organic Modification on Dynamic Compression Properties of Polypropylene/Muscovite Layered Silicate Composites. Mater. Sci. Forum 2014, 803, 282–287.
107. Ding, J.; Huang, Z.; Luo, H.; Qin, Y.; Shi, M. The role of microcrystalline muscovite to enhance thermal stability of boron-modified phenolic resin, structural and elemental studies in boron-modified phenolic resin/ microcrystalline muscovite composite. Mater. Res. Innov. 2015, 19.
108. Kovalevsky, V.; Shchiptsov, V.; Sadovnichy, R. Unique natural carbon deposits of shungite rocks of Zazhogino Ore Field, Republic of Karelia, Russia. In Proceedings of the International Multidisciplinary Scientific GeoConference Surveying Geology and Mining Ecology Management, SGEM, Albena, 30 June–6 July 2016; Volume 1.
109. Xia, L.; Wu, H.; Guo, S.; Sun, X.; Liang, W. Enhanced sound insulation and mechanical properties of LDPE/mica composites through multilayered distribution and orientation of the mica. Compos. Part A Appl. Sci. Manuf. 2016, 81.

110. Zhang, X.; Yuan, L.; Guan, Q.; Liang, G.; Gu, A. Greatly improving energy storage density and reducing dielectric loss of carbon nanotube/cyanate ester composites through building a unique tri-layered structure with mica paper. J. Mater. Chem. A 2017, 5.
111. Michal, O.; Mentlik, V. Influence of Thermal Degradation on the Dielectric Properties of Polymer Composites. In Proceedings of the International Conference on Diagnostics in Electrical Engineering, Diagnostika, Pilsen, Czech Republic, 4–7 September 2018; pp. 1–5.
112. Bae, H.J.; Goh, Y.; Yim, H.; Yoo, S.Y.; Choi, J.W.; Kwon, D.K. Atomically thin, large area aluminosilicate nanosheets fabricated from layered clay minerals. Mater. Chem. Phys. 2019, 221.
113. Lü, R.; Wang, Y.; Wang, J.; Ren, W.; Li, L.; Liu, S.; Chen, Z.; Li, Y.; Wang, H.; Fu, F. Soliton and bound-state soliton mode-locked fiber laser based on a MoS 2 /fluorine mica Langmuir–Blodgett film saturable absorber. Photonics Res. 2019, 7.
114. Geke, M.O.; Shelden, R.A.; Caseri, W.R.; Suter, U.W. Ion exchange of cation-terminated poly(ethylene oxide) chains on mica surfaces. J. Colloid Interface Sci. 1997, 189.
115. Mohammadi, H.; Moghbeli, M.R. Effect of ethylene-1-butene copolymer on tensile properties and toughness of polypropylene/mica/organoclay hybrid nanocomposites. J. Vinyl Addit. Technol. 2019, 25.
116. Fu, Y.; Wang, Y.; Wang, S.; Gao, Z.; Xiong, C. Enhanced breakdown strength and energy storage of PVDF-based dielectric composites by incorporating exfoliated mica nanosheets. Polym. Compos. 2019, 40.
117. Mohammadi, H.; Moghbeli, M.R. Polypropylene/organically modified-grafted mica/organoclay hybrid nanocomposites: Preparation, characterization, and mechanical properties. Polym. Compos. 2019, 40.
118. Wang, B.; Tang, M.; Wu, Y.; Chen, Y.; Jiang, C.; Zhuo, S.; Zhu, S.; Wang, C. A 2D Layered Natural Ore as a Novel Solid-State Electrolyte. ACS Appl. Energy Mater. 2019, 2.
119. Kuznetsov, V.; Ottermann, K.; Helfricht, N.; Kunz, D.; Loch, P.; Kalo, H.; Breu, J.; Papastavrou, G. Surface charge density and diffuse layer properties of highly defined 2:1 layered silicate platelets. Colloid Polym. Sci. 2020, 298.
120. Tani, M.; Fukushima, Y. Properties of organic/inorganic hybrid clay-like polymers with epoxy groups. Kobunshi Ronbunshu 2002, 59.
121. Imai, Y.; Nishimura, S.; Abe, E.; Tateyama, H.; Abiko, A.; Yamaguchi, A.; Aoyama, T.; Taguchi, H. High-modulus poly(ethylene terephthalate)/expandable fluorine mica nanocomposites with a novel reactive compatibilizer. Chem. Mater. 2002, 14.
122. Maiti, P.; Yamada, K.; Okamoto, M.; Ueda, K.; Okamoto, K. New polylactide/layered silicate nanocomposites: Role of organoclays. Chem. Mater. 2002, 14.

123. McNally, T.; Murphy, W.R.; Lew, C.Y.; Turner, R.J.; Brennan, G.P. Polyamide-12 layered silicate nanocomposites by melt blending. Polymer 2003, 44.

124. Sinha Ray, S.; Yamada, K.; Okamoto, M.; Ogami, A.; Ueda, K. New polylactide/layered silicate nanocomposites. 3. High-performance biodegradable materials. Chem. Mater. 2003, 15.

125. Bokobza, L. Elastomeric composites. I. Silicone composites. J. Appl. Polym. Sci. 2004, 93.

126. Zhang, D.; Zhou, C.H.; Lin, C.X.; Tong, D.S.; Yu, W.H. Synthesis of clay minerals. Appl. Clay Sci. 2010, 50.

127. Fukushima, K.; Wu, M.H.; Bocchini, S.; Rasyida, A.; Yang, M.C. PBAT based nanocomposites for medical and industrial applications. Mater. Sci. Eng. C 2012, 32.

128. Fukushima, K.; Tabuani, D.; Camino, G. Poly(lactic acid)/clay nanocomposites: Effect of nature and content of clay on morphology, thermal and thermo-mechanical properties. Mater. Sci. Eng. C 2012, 32.

129. Ruiz-Hitzky, E.; Darder, M.; Wicklein, B.; Fernandes, F.M.; Castro-Smirnov, F.A.; Martín del Burgo, M.A.; del Real, G.; Aranda, P. Advanced biohybrid materials based on nanoclays for biomedical applications. In Proceedings of the Nanosystems in Engineering and Medicine; Choi, S.H., Choy, J.-H., Lee, U., Varadan, V.K., Eds.; SPIE: Incheon, Korean, 2012; Volume 8548, p. 85480D.

130. Vahabi, H.; Sonnier, R.; Otazaghine, B.; Le Saout, G.; Lopez-Cuesta, J.M. Nanocomposites of polypropylene/polyamide 6 blends based on three different nanoclays: Thermal stability and flame retardancy. Polim. Polym. 2013, 58.

131. Ruiz-Hitzky, E.; Aranda, P. Novel architectures in porous materials based on clas. J. Sol-Gel Sci. Technol. 2014, 70, 307–316.

132. Ruiz-Hitzky, E.; Darder, M.; Alcântara, A.C.S.; Wicklein, B.; Aranda, P. Recent advances on fibrous clay-based nanocomposites. Adv. Polym. Sci. 2014, 267.

133. Frindy, S.; Primo, A.; Qaiss, A.E.K.; Bouhfid, R.; Lahcini, M.; Garcia, H.; Bousmina, M.; El Kadib, A. Insightful understanding of the role of clay topology on the stability of biomimetic hybrid chitosan-clay thin films and CO2-dried porous aerogel microspheres. Carbohydr. Polym. 2016, 146.

134. Kojima, Y.; Usuki, A.; Kawasumi, M.; Okada, A.; Kurauchi, T.; Kamigaito, O. Synthesis of nylon 6–clay hybrid by montmorillonite intercalated with ϵ-caprolactam. J. Polym. Sci. Part A Polym. Chem. 1993, 31, 983–986.

135. Jordan, J.W. Organophilic Bentonites. I. Swelling in Organic Liquids. J. Phys. Colloid Chem. 1949, 53, 294–306.

136. Weiss, A. Organic Derivatives of Mica-type Layer-Silicates. Angew. Chem. Int. Ed. Engl. 1963, 2, 134–144.

137. Lan, T.; Kaviratna, P.D.; Pinnavaia, T.J. Mechanism of Clay Tactoid Exfoliation in Epoxy-Clay Nanocomposites. Chem. Mater. 1995, 7, 2144–2150.

138. Vaia, R.A.; Teukolsky, R.K.; Giannelis, E.P. Interlayer Structure and Molecular Environment of Alkylammonium Layered Silicates. Chem. Mater. 1994, 6, 1017–1022.

139. Lagaly, G. Interaction of alkylamines with different types of layered compounds. Solid State Ion. 1986, 22, 43–51.

140. Beyer, G. Nanocomposites: A new class of flame retardants for polymers. Plast. Addit. Compd. 2002, 4, 22–28.

141. Zanetti, M.; Lomakin, S.; Camino, G. Polymer layered silicate nanocomposites. Macromol. Mater. Eng. 2000, 279, 1–9.

142. Unalan, I.U.; Cerri, G.; Marcuzzo, E.; Cozzolino, C.A.; Farris, S. Nanocomposite films and coatings using inorganic nanobuilding blocks (NBB): Current applications and future opportunities in the food packaging sector. RSC Adv. 2014, 4, 29393–29428.

143. Mrah, L.; Meghabar, R. In situ polymerization of styrene–clay nanocomposites and their properties. Polym. Bull. 2020.

144. Ekielski, A.; Żelaziński, T.; Durczak, K. The use of wavelet analysis to assess the degree of wear of working elements of food extruders. Eksploat. Niezawodn. Maint. Reliab. 2017, 19, 560–564.

145. Mościcki, L.; van Zuilichem, D.J. Extrusion-Cooking and Related Technique. In Extrusion-Cooking Techniques; Wiley Online Books; Wiley-VCH Verlag GmbH & Co. KGaA: Weinheim, Germany, 2011; pp. 1–24. ISBN 9783527634088.

146. Vaia, R.A.; Giannelis, E.P. Lattice Model of Polymer Melt Intercalation in Organically-Modified Layered Silicates. Macromolecules 1997, 30, 7990–7999.

147. Chavarria, F.; Shah, R.K.; Hunter, D.L.; Paul, D.R. Effect of melt processing conditions on the morphology and properties of nylon 6 nanocomposites. Polym. Eng. Sci. 2007, 47, 1847–1864.

148. Dennis, H.R.; Hunter, D.L.; Chang, D.; Kim, S.; White, J.L.; Cho, J.W.; Paul, D.R. Effect of melt processing conditions on the extent of exfoliation in organoclay-based nanocomposites. Polymer 2001, 42, 9513–9522.

149. Fornes, T.D.; Paul, D.R. Modeling properties of nylon 6/clay nanocomposites using composite theories. Polymer 2003, 44, 4993–5013.

150. Lertwimolnun, W.; Vergnes, B. Influence of screw profile and extrusion conditions on the microstructure of polypropylene/organoclay nanocomposites. Polym. Eng. Sci. 2007, 47, 2100–2109.

151. Fornes, T.; Yoon, P.; Hunter, D.; Keskkula, H.; Paul, D. Effect of organoclay structure on nylon 6 nanocomposite morphology and properties. Polymer 2002, 43, 5915–5933.
152. Fornes, T.D.; Yoon, P.J.; Keskkula, H.; Paul, D.R. Nylon 6 nanocomposites: The effect of matrix molecular weight. Polymer 2001, 42, 9929–9940.
153. Mittal, V. Polymer layered silicate nanocomposites: A review. Materials 2009, 2, 992–1057.
154. Cabedo, L.; Villanueva, M.P.; Lagarón, J.M.; Giménez, E. Development and characterization of unmodified kaolinite/EVOH nanocomposites by melt compounding. Appl. Clay Sci. 2017, 135, 300–306.
155. Chavarria, F.; Paul, D.R. Comparison of nanocomposites based on nylon 6 and nylon 66. Polymer 2004, 45, 8501–8515.
156. Wang, Z.; Pinnavaia, T.J. Hybrid Organic-Inorganic Nanocomposites: Exfoliation of Magadiite Nanolayers in an Elastomeric Epoxy Polymer. Chem. Mater. 1998, 10.
157. Ganguly, A.; De Sarkar, M.; Bhowmick, A.K. Thermoplastic elastomeric nanocomposites from poly[styrene-(ethylene-co- butylene)-styrene] triblock copolymer and clay: Preparation and characterization. J. Appl. Polym. Sci. 2006, 100.
158. Zhu, L.; Wool, R.P. Nanoclay reinforced bio-based elastomers: Synthesis and characterization. Polymer 2006, 47.
159. Százdi, L.; Pozsgay, A.; Pukánszky, B. Factors and processes influencing the reinforcing effect of layered silicates in polymer nanocomposites. Eur. Polym. J. 2007, 43.
160. Rehab, A.; Akelah, A.; Agag, T.; Shalaby, N. Polyurethane-nanocomposite materials via in situ polymerization into organoclay interlayers. Polym. Adv. Technol. 2007, 18.
161. Chu, D.; Nguyen, Q.; Baird, D.G. Effect of matrix molecular weight on the dispersion of nanoclay in unmodified high density polyethylene. Polym. Compos. 2007, 28.
162. Wilkinson, A.N.; Man, Z.; Stanford, J.L.; Matikainen, P.; Clemens, M.L.; Lees, G.C.; Liauw, C.M. Tensile properties of melt intercalated polyamide 6-Montmorillonite nanocomposites. Compos. Sci. Technol. 2007, 67.
163. Sarkar, M.; Dana, K.; Ghatak, S.; Banerjee, A. Polypropylene-clay composite prepared from Indian bentonite. Bull. Mater. Sci. 2008, 31.
164. Kiliaris, P.; Papaspyrides, C.D.; Pfaendner, R. Polyamide 6 filled with melamine cyanurate and layered silicates: Evaluation of flame retardancy and physical properties. Macromol. Mater. Eng. 2008, 293.
165. Zhang, Y.; Liu, W.; Han, W.; Guo, W.; Wu, C. Preparation and properties of novel natural rubber/organo-vermiculite nanocomposites. Polym. Compos. 2009, 30.

166. Schmidt, D.F.; Giannelis, E.P. Silicate dispersion and mechanical reinforcement in polysiloxane/layered silicate nanocomposites. Chem. Mater. 2010, 22.

167. Lebaron, P.C.; Wang, Z.; Pinnavaia, T.J. Polymer-layered silicate nanocomposites: An overview. Appl. Clay Sci. 1999, 15.

168. Zhu, L.; Wool, R.P. Bio-based elastomers from soy oil and nanoclay. In Nanocomposites with Biodegradable Polymers; Oxford University Press: Oxford, UK, 2011; Volume 9780199581, pp. 189–208.

169. Lipinska, M.; Hutchinson, J.M. Elastomeric epoxy nanocomposites: Nanostructure and properties. Compos. Sci. Technol. 2012, 72.

170. Marega, C.; Causin, V.; Saini, R.; Marigo, A.; Meera, A.P.; Thomas, S.; Devi, K.S.U. A direct SAXS approach for the determination of specific surface area of clay in polymer-layered silicate nanocomposites. J. Phys. Chem. B 2012, 116.

171. Mallakpour, S.; Dinari, M. The effects of reactive organoclay on the thermal, mechanical, and microstructural properties of polymer/layered silicate nanocomposites based on chiral poly(amide-imide)s. J. Therm. Anal. Calorim. 2013, 114.

172. Stojšic, J.; Raos, P.; Kalendova, A. A study of structure and tensile properties of polyamide 12/clay nanocomposites. Polym. Compos. 2016, 37.

173. Ghanbari, A.; Heuzey, M.C.; Carreau, P.J.; Ton-That, M.T. Morphology and gas barrier properties of polymer nanocomposites. Polym. Morphol. Princ. Charact. Process. 2016, 394–417.

174. Rahman, M.R.; Hamdan, S.B.; Hossen, M.F. The effect of clay dispersion on polypropylene nanocomposites: Physico-mechanical, thermal, morphological, and optical properties. In Silica and Clay Dispersed Polymer Nanocomposites; Elsevier: Cambridge, UK, 2018; pp. 201–257.

175. Msekh, M.A.; Cuong, N.H.; Zi, G.; Areias, P.; Zhuang, X.; Rabczuk, T. Fracture properties prediction of clay/epoxy nanocomposites with interphase zones using a phase field model. Eng. Fract. Mech. 2018, 188.

176. Rauschendorfer, J.E.; Thien, K.M.; Denz, M.; Köster, S.; Ehlers, F.; Vana, P. Tuning the Mechanical Properties of Poly(Methyl Acrylate) via Surface-Functionalized Montmorillonite Nanosheets. Macromol. Mater. Eng. 2021, 306.

177. Chang, M.-K.; Wei, H.-L.; Wu, K.-S. The Strength and Thermal Stability of Low-Density Polyethylene Grafted Maleic Anhydride/Montmorillonite Nanocomposites. Adv. Sci. Lett. 2012, 13, 240–244.

178. Kuchta, F.D.; Lemstra, P.J.; Keller, A.; Batenburg, L.F.; Fischer, H.R. Polymer crystallization studied in confined dimensions using nanocomposites from polymers and layered minerals. Mater. Res. Soc. Symp. Proc. 2000, 628.

179. Filippone, G.; Dintcheva, N.T.; Acierno, D.; La Mantia, F.P. The role of organoclay in promoting co-continuous morphology in high-density poly(ethylene)/poly(amide) 6 blends. Polymer 2008, 49, 1312–1322.

180. Tillekeratne, M.; Jollands, M.; Cser, F.; Bhattacharya, S.N. Role of mixing parameters in the preparation of poly(ethylene vinyl acetate) nanocomposites by melt blending. J. Appl. Polym. Sci. 2006, 100, 2652–2658.

181. Liao, B.; Song, M.; Liang, H.; Pang, Y. Polymer-layered silicate nanocomposites. 1. A study of poly(ethylene oxide)/Na+-montmorillonite nanocomposites as polyelectrolytes and polyethylene-block-poly(ethylene glycol) copolymer/Na+-montmorillonite nanocomposites as fillers for reinforcement of po. Polymer 2001, 42.

182. Lim, S.K.; Lim, S.T.; Kim, H.B.; Chin, I.; Choi, H.J. Preparation and Physical Characterization of Polyepichlorohydrin Elastomer/Clay Nanocomposites. J. Macromol. Sci. Phys. 2003, 42.

183. Li, X.; Mishra, J.K.; Seul, S.D.; Kim, I.; Ha, C.S. Microstructure and properties of poly (butylene terephthalate) based nanocomposites. Compos. Interfaces 2004, 11, 335–346.

184. Ahmadi, S.J.; Huang, Y.D.; Li, W. Synthetic routes, properties and future applications of polymer-layered silicate nanocomposites. J. Mater. Sci. 2004, 39.

185. Song, L.; Hu, Y.; Tang, Y.; Zhang, R.; Chen, Z.; Fan, W. Study on the properties of flame retardant polyurethane/organoclay nanocomposite. Polym. Degrad. Stab. 2005, 87.

186. Li, J.; Zhao, L.; Guo, S. Ultrasonic preparation of polymer/layered silicate nanocomposites during extrusion. Polym. Bull. 2005, 55.

187. Chang, M.-K. Mechanical properties and thermal stability of low-density polyethylene grafted maleic anhydride/montmorillonite nanocomposites. J. Ind. Eng. Chem. 2015, 27, 96–101.

188. Sinha Ray, S.; Okamoto, M. Biodegradable polylactide and its nanocomposites: Opening a new dimension for plastics and composites. Macromol. Rapid Commun. 2003, 24.

189. Vlasveld, D.P.N.; Daud, W.; Bersee, H.E.N.; Picken, S.J. Continuous fibre composites with a nanocomposite matrix: Improvement of flexural and compressive strength at elevated temperatures. Compos. Part A Appl. Sci. Manuf. 2007, 38.

190. Akbari, B.; Bagheri, R. Deformation mechanism of epoxy/clay nanocomposite. Eur. Polym. J. 2007, 43.

191. Yamagata, S.; Iida, J.; Watari, F. FRP Esthetic Orthodontic Wire and Development of Matrix Strengthening with Poly(methyl methacrylate)/Montmorillonite Nanocomposite. In Handbook of Polymernanocomposites. Processing, Performance and Application; Springer: Berlin/Heidelberg, Germany, 2014; pp. 319–328. ISBN 9783642386497.

192. Tasan, C.C.; Kaynak, C. Mechanical performance of resol type phenolic resin/layered silicate nanocomposites. Polym. Compos. 2009, 30.